Selective PARP inhibition via benzamide is neuroprotective from AMPA-induced excitotoxic cell death of rat cerebellar Purkinje neurons

by

William M. Henne

A SENIOR THESIS

for the

UNIVERSITY HONORS COLLEGE

Submitted to the
University Honors College
at Texas Tech University in
partial fulfillment of the
requirement for
the degree designation of

HIGHEST HONORS

MAY 2005

Approved by:

_____ 4/28/05

FACULTY MENTOR (Jean Strahlendorf, Ph.D.) Date
Department of Physiology

_____ 5/10/05

DR. GARY M. BELL Date
Dean, University Honors College

Selective PARP inhibition via benzamide is neuroprotective from AMPA-induced excitotoxic cell death of rat cerebellar Purkinje neurons

W. M. Henne[1], H. Strahlendorf[2], and J. Strahlendorf[1]
[1]Department of Physiology, Texas Tech University Health Sciences Center, Lubbock, TX 79430, USA
[2]Department of Pharmacology and Neuroscience, Texas Tech University Health Sciences Center, Lubbock, TX 79430, USA

Abstract

Programmed cell death (PCD) is a critical behavior of cells comprising multicellular eukaryotes. However, excessive PCD in the brain often yields neurodegeneration, and AMPA-receptor-mediated excitotoxicity has been linked to PCD in Purkinje neurons (PNs) of the cerebellum. Recently, several key enzymes were shown to mediate AMPA-induced PCD in PNs, but the role of an emergingly-important death enzyme—known as *P*oly (*A*DP-*r*ibose) *P*olymerase (PARP)—has yet to be analyzed in PNs. This study investigated the importance of PARP in AMPA-induced PCD in cerebellar PNs *in situ* via the use of a selective PARP inhibitor, known as benzamide. Specifically, morphological studies were performed analyzing AMPA-induced changes of PNs via toluidine blue staining. Fluorescent confocal imaging also investigated the locale and expression levels of PARP. Data indicated that the addition of benzamide to AMPA-insulted cerebellar slices resulted in neuroprotection, yielding fewer pathomorphic PNs. In addition, cerebellar slices treated with benzamide alone demonstrated only mild toxicity, suggesting benzamide itself is not significantly pathogenic. Finally, fluorescent tagging of PARP in PNs confirms the suppression of PARP presence in PNs treated with benzamide. Altogether, these findings suggest that PARP plays a critical role in the molecular mechanisms of AMPA-induced PCD in cerebellar PNs, and PARP inhibition may act

as a neuroprotectant. Such knowledge may prove invaluable to therapies designed to prevent or moderate the neurodegenerative effects of AMPA-receptor associated brain diseases, such as seizure-induced PCD.

Key words: programmed cell death, AMPA-receptor-mediated excitotoxicity, cerebellar Purkinje neurons, PARP

Introduction

Programmed cell death (PCD) is an essential process of multi-cellular organisms. Unneeded or damaged cells are edited out of tissues, preserving the integrity of the organism. However, uncontrolled PCD has been associated with many human diseases, including Alzheimer's and multiple sclerosis [2, 8].

Intracellular PCD mechanisms are initiated in many ways. One such initiator can be an excitotoxic concentration of a neurotransmitter. Glutamate, the chief excitatory neurotransmitter of the central nervous systems, has been implicated in excitotoxic PCD. High levels of glutamate can over-stimulate the AMPA receptor, a type of glutamate receptor present on neurons. Previous studies have identified key protein mechanisms, such as caspase cascades, involved in AMPA-induced PCD [5, 9, and 4]. However, these studies have yet to elucidate the importance of the enzyme *P*oly (*A*DP-*r*ibose) *P*olymerase (PARP) in the process of AMPA-induced PCD.

PARP, a 118kDa enzyme present in all examined eukaryotic life except yeast, was originally known to play a key role in DNA repair [3]. However, emerging evidence suggests

this enzyme may play a key role in the execution of caspase-independent PCD [reviewed in 6]. Studies in our lab are currently investigating caspase -dependent and -independent mechanisms that may be activated in response to AMPA-insult in cerebellar Purkinje Neurons (PNs), and thus investigating the importance PARP in our PCD model is of critical importance to our elucidation of the AMPA-induced PCD mechanism.

Specifically, PARP is known to associate with ADP-ribose molecules in the nucleus of a PCD–initiated cell, and it subsequently polymerizes these ADP-riboses, thus depriving the cell of essential resources for mRNA transcription and energy manufacturing, as well as perpetuating the cell death signal to downstream PCD enzymes [6]. In caspase mediated PCD, caspase-3 cleaves PARP, thus deactivating it [10].

Thus, the purpose of this project is to investigate the importance of PARP in the AMPA-induced excitotoxic PCD of rat cerebellar Purkinje neurons. Experiments were conducted on cerebellar tissue slices by adding a 30μM concentration of AMPA agonist to these slices—this induced an excitotoxic PCD response. Control slices received no AMPA agonist. In addition, some samples were exposed to the PARP inhibitor benzamide as well as the AMPA agonist, and others received the PARP antagonist alone as a control [1]. The tissue slices were then fixed at regular intervals during the experiment. These fixed tissues were stained, displaying the morphology of the PNs. By analyzing the pathomorphology of the PNs exposed to benzamide and AMPA agonist, we determined if inhibiting PARP played a neuro-protective role by inhibiting AMPA-induced PCD. Fluorescent antibodies specific for PARP p85 fragment, which is generated when active PARP is cleaved by caspase-3, were used to identify the locale of

PARP in the PNs, as well as PARP's relative expression levels in PNs exposed to AMPA and benzamide.

Thus, the chief hypothesis of this project is: PARP is of critical importance in the AMPA-induced PCD of cerebellar PNs, and inhibition of PARP will suppress the PCD mechanism initiated by AMPA-insult, subsequently yielding more healthy-appearing PNs after their exposure to the excitotoxic AMPA agonist. As a corollary, we would also predict a corresponding decrease in fluorescently labeled PARP p85 fragment in PNs exposed to benzamide, correlating with benzamide's suppression of PARP.

Methods

AMPA-addition experiment

Dark Cell Degeneration, a type of PCD, was induced by AMPA stimulation of PNs in cerebellar slices as previously described [9]. Briefly, postnatal (8 to 12 days old) Sprague-Dawley strain rats (Sasco Labs) of either sex were decapitated between the C1 and C2 vertebrae and surgery was preformed to remove the brain. At least three rats were used per experiment. The cerebellum was excised and sliced sagittally into 400μm portions using an oscillating tissue slicer (Frederick Haer and Co). The tissue was placed in Erlenmeyer flasks and submerged in 20mL artificial cerebrospinal fluid (aCSF) that was oxygenated with 95% O_2 and 5% CO_2 gas. aCSF components include (in mM): NaCl (120), KCl (2), KH_2PO_4 (1.2), $MgSO_4$ (1.2), $CaCl_2$ (2), $NaHCO_3$ (26), and glucose (11); Osmolarity = 285-295mOsm, pH 7.4.

Cerebellar slices were exposed to 30μM AMPA concentrations for a 30 minute "trigger" phase. Handling control (HCNTL) slices received no AMPA. Slices were then transferred to

newly oxygenated aCSF without AMPA for the "expression" phase. Some control slices also received this benzamide treatment with no AMPA treatment. Samples exposed to 5mM benzamide received treatment 20 minutes prior to AMPA exposure, during the 30 minute AMPA exposure, and during the 90 minute post-AMPA "expression" phase. The aCSF was replaced every 60 minutes of the "expression" phase to maintain adequate oxygenation. Tissue slices were removed at 90 minutes into "expression phase" and immediately fixed in 4% paraformaldehyde. After 24 hours in paraformaldehyde, slices were stored in 30% sucrose-PBS.

Slices were cut further into 12µm sagittal sections using a Tissue-Tek® Cryostat (Miles) and adhered to gelatin-covered glass cover slips with Tissue Freezing Medium (Triangle Biomedical Sciences) for subsequent immunohistochemical labelling. Complementing 6µm slices were adhered to gelatin-treated microscope slides for morphological examination, and were stained with toluidine blue.

Morphological Assessment of Cerebellar PNs

The toluidine blue-stained cerebellar sections were examined under a light microscope at 20X and 40X objective magnifications. A PN-rich field-of-view was found for each experimental group (handling control, AMPA 30µm-exposed, AMPA 30µm-exposed + 5mM benzamide, and handling control + 5mM benzamide) at 20X magnification, and all of the PNs in that field were morphologically assessed. Specifically, PNs were placed into 3 categories: healthy, DCD, and edematous. Healthy PNs appeared plump, lightly stained, with intact dendritic and axonal extension and a clear nucleus. By contrast, DCD-appearing PNs demonstrated a dark, shrunken, and mis-shapen appearance with shriveled extensions and no clear nucleus. Edematous PNs were identified by no somal body, but rather by an empty space

where the PN "exploded" following traumatic cell death (possibly from surgical procedures). High numbers of edematous PNs suggested tissue slices that received traumatic post-surgical treatment, and were not included in morphological counts. Three different experimental dates were examined, each containing all four treatments of the study (N=3).

PARP fluorescent labeling via immunohistochemistry

A three-day immunohistochemical protocol was done using PARP-specific primary antibodies that were detected using fluorescently tagged secondary antibodies. During day one, sections were washed in PBS and treated with acetone at -20°C to enhance tissue antigenicity, then permeabilized overnight in 0.5% Triton X-100 at 4°C. On day two, slices were treated with a blocking solution (0.5% Triton X-100 and 10% normal goat serum in PBS), rinsed in PBS, and then washed in PBS again. Slices were then exposed overnight to the primary antibody: rabbit polyclonal anti-PARP p85 fragment (1:100, Promega Corporation). This antibody labels the p85 fragment generated when PARP is cleaved by Caspase-3 during programmed cell death. On day three, slices were rinsed in PBS and treated with an Alexa 488-tagged goat anti-rabbit secondary antibody (1:250, Molecular Probes) for 2 hours, then rinsed in PBS. Slices were then rinsed three times with deionized water, air dried, and mounted with anti-fade medium.

Laser scanning confocal microscopy (LSCM)

Images of PNs were obtained from the control and AMPA-treated sections using a BioRad MRC 1024 laser scanning confocal imaging system equipped with Argon-Krypton lasers and coupled to an Olympus IX70 inverted microscope with a 1.4 numerical aperture 60X oil-immersion objective. The imaging system was controlled by Laser Sharp software (version 3.2; BioRad, Hercules, CA). Alexa 488-labeled slices were excited by 488 nm laser light and images

were acquired using a 522 nm emission filter with a bandwidth of ± 35 nm. Settings of the confocal microscope were optimized for imaging each experiment and then equivalently applied to all control and treated sections. Laser power and PMT gain were adjusted to insure that even the brightest fluorescence was below saturation (eight bit), and the iris setting was routinely set at 2 (equivalent to approximately a one micron optical section). Optical fields were chosen randomly and scanned at 512 X 512 pixel resolution.

To examine and quantitate differences in fluorescence from immunostained sections, images were imported into Image Tool, a quantitative software program that measures the pixel intensity of a user-defined circumscribed area (University of Texas Health Sciences Center, San Antonio, TX; currently available as Scion Image, Scion Corporation, Frederick, MD). All comparisons were made from images obtained with identical settings of the confocal microscope. Fluorescent intensities from two or three areas within cells-of-interest (representing approximately 60% of the cytosolic regions within each cell) were analyzed in individual PNs from control and AMPA-treated groups. PNs that exhibited morphological evidence of DCD in response to AMPA were chosen for analyses. This raw fluorescent data was averaged and graphed in Figure 3. All quantitation was performed without prior knowledge of the treatment.

Statistics

Statistical analyses were performed using Microsoft Excel or PSI-Plot (Poly Software International, Pearl River, NY). For two group comparisons, we employed the t-test for groups with unequal variances. The significance level was set at $p \leq 0.05$.

Results

Results Summary

Cerebellar PNs insulted with 30μM AMPA agonist demonstrated prevalent pathomorphologies previously identified as DCD [9]. This shrunken, dark-stained morphology appears in stark contrast to the healthy morphology seen in the handling control samples not receiving AMPA. In addition, when the PARP inhibitor benzamide was added co-currently with 30μM AMPA, the number of healthy PNs increased. Subsequently, there was a correlative decrease in DCD morphology in these samples. Handling control samples receiving benzamide treatment without AMPA also demonstrated high levels of healthy PNs. Edematous PNs—represented by empty pockets in the tissue where the PNs lysed due to excess trauma during surgery of over-excitation—were seen in low occurrence throughout all treatments. Fluorescent tagging of PARP confirmed its presence in the PN cytosol and its decreased presence when PNs were exposed to benzamide.

30μM AMPA insult facilitated DCD in PNs

When cerebellar PNs were insulted with 30 minutes of 30μM AMPA agonist, then left in aCSF for 90 minutes, over 63% of the PNs demonstrated DCD-like morphology (Figure 1). DCD neurons demonstrated darkened somal staining, shrunken cell shape, and degraded dendritic and axonal extensions on their bodies (Figure 2, panel C), and appeared in stark contrast to healthy PNs, which continued to be plump, lightly stained, and bristling with a main axonal extension and a dendritic tree (Figure 2, panel A). About 33% of the PNs in AMPA-

insulted slices did demonstrate healthy morphology. Edematous PNs were in extremely low occurrence, present in only 3% of the PN population.

PARP Inhibitor benzamide treatment suppressed DCD morphology

When 5mM benzamide was added to cerebellar slices 20 minutes prior to the AMPA insult, during the 30 minute AMPA insult, and during the 90 minute post-AMPA expression period, the PN population demonstrated greater numbers of healthy PNs than with AMPA alone (Figure 2, panel D). Almost 49% of the PNs in the 30μM AMPA + 5mM benzamide-treated slices had healthy morphologies, and only 42% demonstrated DCD morphology (Figure 1). Again, edematous PNs were rare, constituting only about 9% of the population (Figure 1).

Benzamide was not neurotoxic

When PNs were exposed to 5mM benzamide treatment without any AMPA insult, over 61% of the PNs retained their healthy morphology (Figure 1). Their morphology correlated to the healthy morphology seen in handling control samples alone (Figure 2, panel B). About 37% appeared to suffer a DCD-like morphology, and only 2% edematous PNs were observed. These percentages were essentially equivalent to those from handling control slices.

Fluorescent tagging confirmed benzamide suppression of PARP

Fluorescent tagging of PARP in PNs, and the subsequent imaging of the PNs via LSCM, demonstrated that PARP resided in the cytosol of PNs (Figure 3). Whereas AMPA exposed PNs demonstrated high levels of PARP as compared to handling control (Figure 3a, A & B), the

addition of 5mM benzamide suppressed PARP fluorescent signal (Figure 3a, C & D). In both AMPA-exposed and handling control PNs exposed to benzamide, PARP levels fell to significantly under those seen in AMPA-insulted PNs alone (Figure 3b).

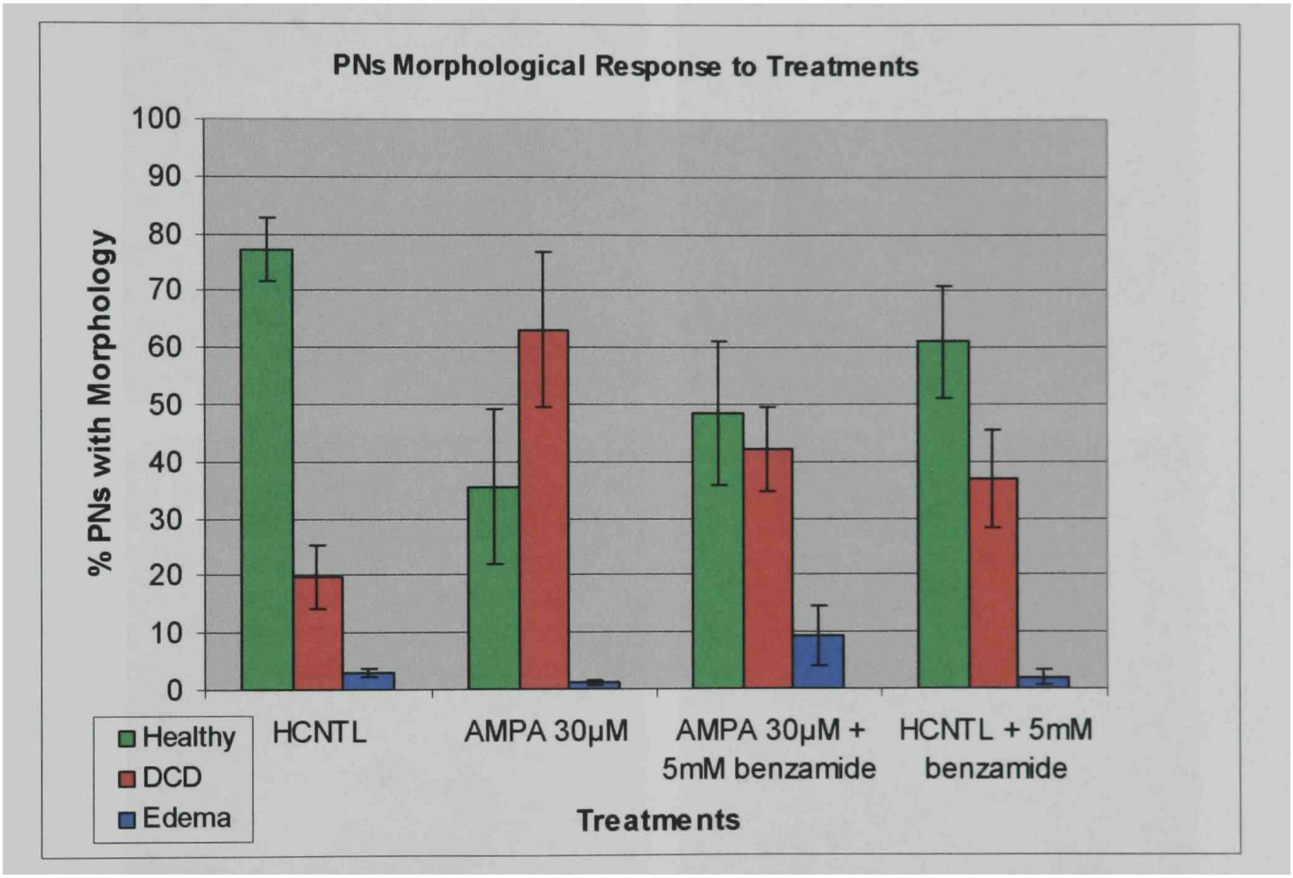

Figure 1. Graph of the percentage of different PN morphologies in cerebellar slices exposed to various treatments. The HCNTL (handling control, which did not receive AMPA, nor benzamide treatment) demonstrated mostly healthy morphology of PNs. In contrast, 30µM AMPA induced mostly DCD-appearing PNs. 30µM AMPA + 5mM benzamide resulted in a return to mostly healthy PNs, although about 42% of the PNs retained their DCD morphology. HCNTL + 5mM benzamide demonstrated mostly healthy PNs. N=3.

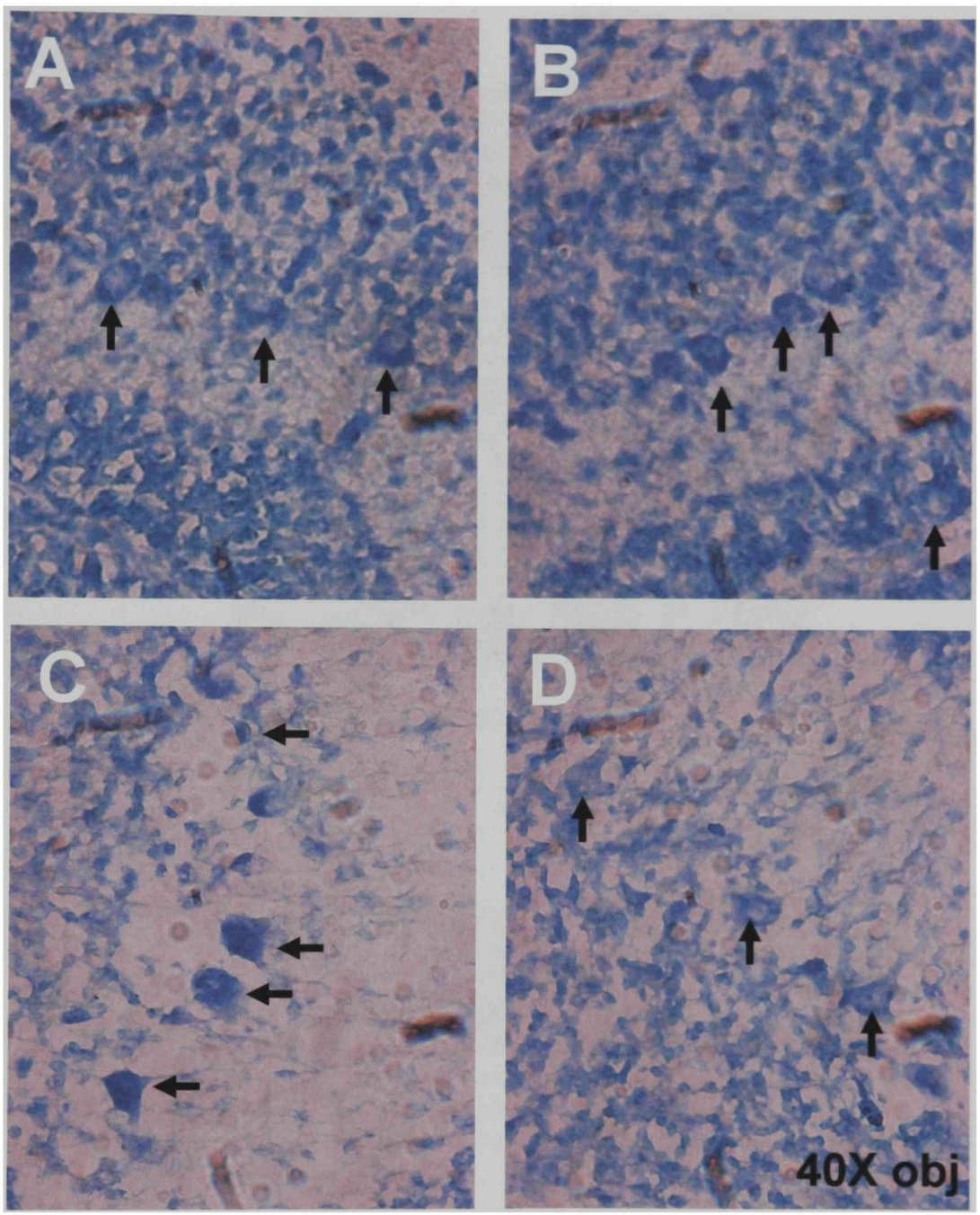

Figure 2. Light microscope images at 40X objective magnification of toluidine blue-stained PNs. The handling control PNs (panel A) demonstrate plump, round soma shape and a distinct nuclear clearing, indicative of healthy PNs. Handling control slices of the cerebellum exposed to 5mM benzamide also demonstrate healthy PNs, again showing plump PNs with clearly present nuclei (panel B). In contrast, 30μM AMPA-exposed PNs of the cerebellum demonstrate shrunken, darkly stained PNs without clearly present nuclei, indicative of DCD (panel C). However, 30μM AMPA-exposed PNs that also receive 5mM benzamide treatment demonstrate healthy morphology, similar to handling control PNs (panel D). Arrows indicate PNs of interest.

a)

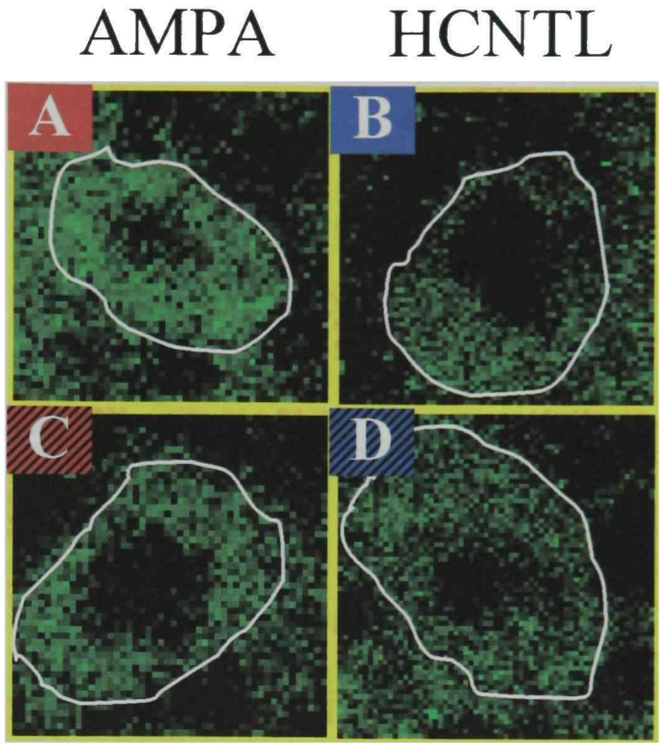

b)

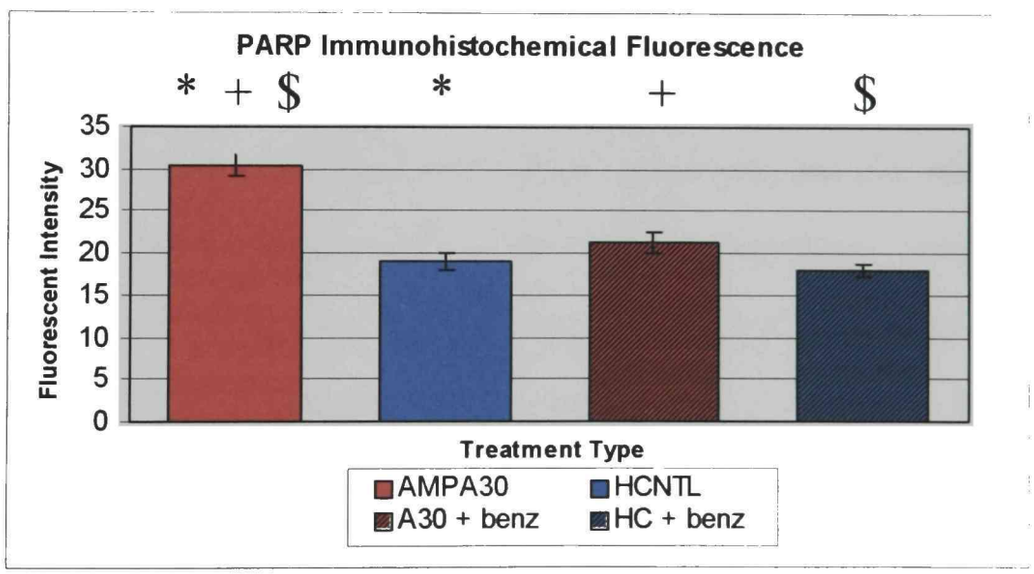

Figure 3. **a)** Images of individual PNs under LSCM at 60X, fluorescently labeled with anti-PARP antibody. The PNs have been outlined in white. The AMPA exposed PN demonstrated significant PARP fluorescence in the cytosol (A), whereas the handling control PN demonstrated less PARP fluorescence (B). 5mM benzamide treatment in samples C and D caused less PARP fluorescent signal in PN, both in the PN also treated with AMPA (C), and the handling control + benzamide (D). **b)** The chart below the figures is the quantized PARP fluorescent intensity values for the PNs from above. Quantitation confirms that PARP intensity is significantly greater in AMPA-exposed PNs without benzamide, and that benzamide reduces AMPA-related PARP fluorescent intensity significantly. The *, +, and $ indicate statistical differences with an unpaired t-test, $p<0.05$.

Discussion

Any agent that suppresses the expression of neurotoxic morphologies in insulted neurons may be construed to have a neuroprotective, and potentially therapeutic, use in treating neurodegenerative diseases. The PARP inhibitor benzamide, based on the results presented here, appeared to afford neuroprotection against AMPA-induced excitotoxic cell death of cerebellar PNs. It can subsequently be concluded that PARP plays an important role in AMPA-induced PCD.

A 30μM AMPA insult generated significant increases in DCD morphology among the PNs of our cerebellar samples, suggesting that this AMPA insult initiated a neurodegenerative cell death cascade. Such AMPA-induced PCD cascades have been established in other studies [5, 9, and 4], but the importance of PARP was not yet elucidated in the mechanism. Our studies using the PARP inhibitor benzamide attempted to address this knowledge gap.

When 5mM benzamide was administered before, concurrently, and after AMPA-insult to cerebellar slices, the PN population demonstrated more healthy morphologies, correlating with a dramatic decrease in DCD morphology. This suggested that PARP was involved with the neurodegenerative cell death mechanism initiated by AMPA-insult, and by halting the enzymatic activity of PARP via benzamide, this PCD process was critically suppressed. A portion of PNs did continue to manifest DCD morphology (about 42%), and this suggested either a limited neuroprotective effect of benzamide, a need for an increased concentration during benzamide treatment, or even a separate PCD mechanism in these cells independent of PARP involvement. It is important to also note the increased presence of edematous PNs in the samples treated with 30μM AMPA and 5mM benzamide, which may be due to slight trauma on the tissue during

processing, or even a manifestation of another form of cell death since PARP was inhibited in these insulted PNs (see below).

When benzamide alone was administered to cerebellar PNs, most (about 61%) retained their healthy morphology. However, even with exposure to 5mM benzamide alone, about 37% of the PNs still appeared to have DCD-like morphology. This may have been due to trauma involved in the surgical removal of the cerebellum from the rat brain, or even mild excitotoxicity from benzamide, and must be further investigated. Since PARP is known to be involved in DNA repair and maintenance, its inhibition during non-PCD events may facilitate cell pathology, which morphologically would look similar to DCD. However, this amount of DCD is similar to the level seen in handling control slices that were not treated with benzamide, and suggests the effect may be from slice preparation alone. It is also important to note that DCD-like morphology does not directly correlate with AMPA-induced DCD; morphological assessment is an imperfect technique, and the appearance of two similar cell morphologies does not mean they originate from the same molecular mechanism.

As stated above, the 30μM AMPA + 5mM benzamide samples indicated a slightly increased prevalence of edematous PN morphology as compared to handling control, handling control + 5mM benzamide, and 30μM AMPA alone samples. Different forms of PCD often manifest vastly different cell morphologies, and *necrotic-like* forms of PCD tend to cause cell swelling and bursting that appear edematous in nature [7 for review]. These necrotic mechanisms are not passive forms of cell death, however, but rather part of an active mechanism of PCD that functions as an alternative to classical apoptosis. PARP, due to its involvement with key mediators of caspase independent cell death, may act as a "molecular switch" by which its

inhibition may force PNs into a form of this necrotic PCD, which manifests as edematous morphology. Therefore, 30μM AMPA potentially induced several PCD cascades in the PNs, and 5mM benzamide treatment filtered their expression of PCD mechanisms into a necrotic form. Thus, we did not see high levels of edematous morphology in handling control + 5mM benzamide treatment, because although PARP was inhibited, the cells were not actively insulted by AMPA to initiate these various PCD mechanisms.

Fluorescent imaging of PARP provided confirmation of the suppressive ability of benzamide to PARP's presence in the cytosol. AMPA-treated PNs demonstrated high levels of PARP p85 fluorescence in their cytosol as compared to handling control PNs, suggesting large amounts of PARP were being activated via AMPA-induced PCD, and were subsequently cleaved by caspase-3 into the labeled PARP p85 fragment. In contrast, this high level of PARP was not seen in AMPA-exposed PNs also treated with 5mM benzamide, and thus less PARP was activated to be cleaved by caspase-3. Handling control PNs also receiving benzamide have similarly low levels of PARP fluorescence. This suggests that benzamide suppresses PARP expression or activation in PNs, which probably leads directly to benzamide's neuroprotective effects in these PNs.

As for the benzamide's molecular mechanism of PARP inhibition, it has been suggested that benzamide can inhibit the transfer of ADP from one biological molecule to another [11]. Since PARP functions as a poly-ADP polymerase in its active form, and this activity is associated with cellular reducing power starvation during PCD, benzamide may suppress the ADP polymerization of PARP during AMPA-induced excitotoxic PCD in cerebellar PNs.

It must be noted that the high degree of error between the three morphological experimental replicates has resulted in a lack of statistical significance in our studies. As such, more replicates are being planned before the conclusion of this project, which will (hopefully) eliminate much of the standard error and allow statistically significant levels of neuroprotection to be seen in AMPA-insulted PNs treated with benzamide.

Acknowledgements

I would like to thank the Texas Tech University Honors College, particularly Joel Walker, with his assistance in the establishment of this project as my senior thesis. I would also like to thank Jennifer Attridge, Somini Oomman, Velvet Lee Finckbone, Bobby Mansouri, Margarita Medina, Taurek Zeitini, Rick Bliss, and all members of the Dr. Jean Strahlendorf research team. Special thanks go to my Research Mentor, Dr. Jean Strahlendorf, and Research Reviewer, Dr. Howard Strahlendorf, for all of their patience and efforts in my research endeavors.

Works Cited

1) Bryant HE, Helleday T. 2004. Poly(ADP-ribose) polymerase inhibitors as potential chemotherapeutic agents. 32(6): 959-61.

2) Chan SL, Griffin WS, Mattson MP. 1999. Evidence for caspase-mediated cleavage of AMPA receptor subunits in neuronal apoptosis and Alzheimer's disease. *Jour. Neurosci. Res.* 57(3): 315-23.

3) Durkacz BW, Omidiji O, Gray DA, Shall S. 1980. (ADP-ribose)n participates in DNA excision repair. *Nature.* 5747: 536-9.

4) Garthewaite G, Garthewaite J. 1991. AMPA Neurotoxicity in Rat Cerebellar and Hippocampal Slices: Histological Evidence for Three Mechanisms. *Eur. J. of Neuroscience.* 3: 715-728.

5) Garthwaite G, Garthwaite J. (1991) Mechanisms of AMPA Neurotoxicity in Rat Brain Slices. *Eur J Neurosci.* 3(8): 729-736.

6) Hong SJ, Dawson TM, Dawson VL. 2004. Nuclear and mitochondrial conversations in cell death: PARP-1 and AIF signaling. *Trends. Pharm. Sci.* p. 259-64.

7) Leist M, Jaattela M. 2001. Four deaths and a funeral: from caspases to alternative mechanisms. *Nat Rev Mol Cell Biol.* 2(8): 589-98.

8) Pitt D, Werner P, Raine CS. 2000. Glutamate excitotoxicity in a model of multiple sclerosis. *Nat. Med.* 6(1): 67-70.

9) Strahlendorf J, Box C, Attridge J, Diertien J, Finckbone V, Henne WM, Medina MS, Miles R, Oomman S, Schneider M, Singh H, Veliyaparambil M, Strahlendorf H. (2003) AMPA-induced dark cell degeneration of cerebellar Purkinje neurons involves activation of caspases and apparent mitochondrial dysfunction. 994(2): 146-59.

10) West JD, Ji C, Marnett LJ. 2005. Modulation of DNA fragmentation factor 40 nuclease activity by poly (ADP-ribose) polymerase-1. *J Biol Chem.* Feb 9; [Epub ahead of print]. PMID: 15703174.

11) Whish WJ, George AM, Lunec J, Cramp WA, Brennan S, Lewis PD. 1986. The effects of benzamide ADP-ribosyl transferase inhibitors on cell survival and DNA strand-break repair in irradiated mammalian cells. *Int J Radiat Biol Relat Stud Phys Chem Med.* May; 49(5): 783-98.